

Drought hazard assessment using GIS techniques in the Banská Bystrica region

Kamila Hodasová, Dávid Krčmář, Martin Zatlakovič & Ivana Ondrejková

Department of Engineering Geology, Hydrogeology and Applied Geophysics, Faculty of Natural Sciences, Comenius University Bratislava, Ilkovičova 6, 842 15, Bratislava, Slovakia; hodasova11@uniba.sk

AGEOS

Abstract: Drought research is currently a topical issue, given that drought is an extreme phenomenon, the consequences of which threaten nature, the landscape, and society. The lack of precipitation and a subsequent reduction in water runoff threatens drinking water supplies, the dries up streams and springs, or the deteriorates the quality of natural waters. The aim of the study is the assessment of drought hazard in the Banská Bystrica region. Initially, the standardized precipitation index (SPI) was calculated for the period 1981–2021 for 34 gauging stations in the Banská Bystrica region. It was possible to examine temporal drought patterns through the SPI indices. A certain correlation is evident among the assessed stations, with variations primarily attributed to differences in altitude and the different distribution of precipitation. To assess the spatial distribution of drought hazard, a probability map of drought occurrence, referred to as the drought index (DHI) map, was created. The DHI map was created using tools in the ArcGIS environment: inverse distance weighted (IDW) interpolation, natural break method and map algebra. The drought hazard map was categorized into 4 classes, while 12.42 % of the territory is in a very high degree of drought probability. Temporal and spatial aspects of drought represent an important component in the assessment of extreme climate events. A scientific approach based on the assessment of drought hazard, vulnerability, and risk in the environment of GIS systems creates a useful tool aimed at quantifying and predicting drought within regional systems.

Key words: Drought hazard, standardised precipitation index, Banská Bystrica Region, GIS, IDW

1. INTRODUCTION

Drought, as one of the most fundamental natural hazards, poses a significant threat to biodiversity, ecological balance, and the environment, with profound impacts on human communities and their economic stability. In the context of the continuously evolving climate system and extreme meteorological events, the development of sophisticated tools for the quantification and assessment of drought becomes imperative to gain a deeper understanding of its scope, intensity, and potential consequences.

The term “hazard” encapsulates the natural occurrence of drought (Wilhite, 2005). Drought hazard can be defined as the probability of the intensity and frequency of drought in a given area or the likelihood of drought occurrence. The drought hazard index is determined through the statistical analysis of drought indices such as the Standardized Precipitation Index (SPI) (Alamdarloo et al., 2020).

The SPI is a widely utilized index that provides robust estimates of drought intensity, extent, and spatial distribution. The SPI is a drought index first developed by T. B. McKee, N.J. Doesken, and J. Kleist in 1993 (McKee et al., 1993). Integrated into drought monitoring and management systems, the SPI is particularly effective in hydrological drought assessments over extended time scales (over 6 months) (Asrari et al., 2012).

Given the contemporary climate changes leading to more frequent and intense extreme conditions, it is essential to investigate and compare the effectiveness of the drought hazard index in various geographic regions, including Greece (Tsesmelis et al., 2022), China (Bin et al., 2011), Turkey (Dabanli, 2018), Iran (Nasrollahi et al., 2018), Jordan (Hajar et al., 2019), Bangladesh (Rahman & Lateh, 2016), Hungary (Domonkos, 2003), and

Spain (Lana et al., 2021). Drawing insights from existing studies utilizing this methodology across diverse global regions allows us to assess its reliability and precision. To illustrate, Salvacion (2022) applied the SPI index to assess drought in the Philippines using TerraClimate data, providing long-term monthly precipitation information.

The Slovak Hydrometeorological Institute (SHMI) launched the monitoring of meteorological and soil drought in 2015, later expanding to include the monitoring of groundwater and surface water conditions, along with assessing the impacts of drought in 2017. This monitoring utilizes three drought indices – SPEI (Standardised Precipitation and Evapotranspiration Index), SPI, CMI (Crop Moisture Index) – with their trends visualized in graphs and updated weekly on the SHMI website.

A study by Rozkošný et al. (2022) analysed drought occurrences in the Orava region from 2015 to 2021, considering precipitation deficit and soil moisture, and assessed the subsequent impact on forest stands. Turňa et al. (2021) evaluated the drought situation in Slovakia in 2020 using SPEI and CMI indices. Janáčová et al. (2018) examined meteorological drought in lowland regions of Slovakia from 1981 to 2010 employing SPI indices. Portela et al. (2015) conducted a thorough drought analysis in Slovakia utilizing SPI. Nagy et al. (2020) assessed the trend analysis of drought indices in eastern Slovakia.

The objective of this study is to employ SPI indices and GIS systems as tools for drought assessment in the Banská Bystrica region, with a focus on their application in the context of climate change. This approach aims to provide valuable insights for effective drought management and prevention of adverse impacts. Drought hazard serves as the starting point for further analyses and is indispensable in calculating drought risk analysis.

2. STUDY AREA

The Banská Bystrica Region, with an area of 9,455 km², is the largest territorial unit in Slovakia (Fig. 1). The region is administratively divided into 13 districts: Banská Bystrica, Banská Štiavnica, Brezno, Detva, Krupina, Lučenec, Poltár, Revúca, Rimavská Sobota, Veľký Krtíš, Zvolen, Žarnovica, and Žiar nad Hronom. There are a total of 516 municipalities in the region, including 24 towns.

The Banská Bystrica Region is characterized by its geomorphological diversity, ranging from the high mountain ridges of the Nízke Tatry Mts. in the north, through alternating mountain massifs and valleys in the central part, to undulating and flat locations in the southern part of the region. In the region, there are five national parks: Nízke Tatry, Veľká Fatra, Muránska planina, Slovenský Raj, and Slovak Karst. The highest peak in the Banská Bystrica Region is Ďumbier Mount (2,043 m a.s.l.) located in the Nízke Tatry Mts. in the Brezno district. The lowest point in the region is in the cadastre of Ipelské Predmostie village (126 m a.s.l.) in the Veľký Krtíš district (Atlas of Landscape SR, 2002).

In Figure 1, gauging stations are labelled with numbers. The gauging stations and their altitudes are listed in the Table 1.

The morphologically diverse terrain of the region also influences its climatic conditions, characterized by instability and variability. The northern part of the territory belongs to a cold climatic zone, with the occurrence of temperature inversions in the valleys. The Southern Slovak and Zvolen basins have warmer and drier weather (Atlas of Landscape SR, 2002).

Hydrological conditions in the Banská Bystrica Region are influenced by natural divisions. The territory is a part of three partial catchments – the Hron river catchment, the Ipel' river catchment, and the Slaná river catchment, with a total length of watercourses in the region being 4,977 km. The Hron River, originating in the region, is its most significant and longest river, draining the entire northwest part of the region. The Ipel' and Slaná rivers form the border with Hungary. The Hron Valley

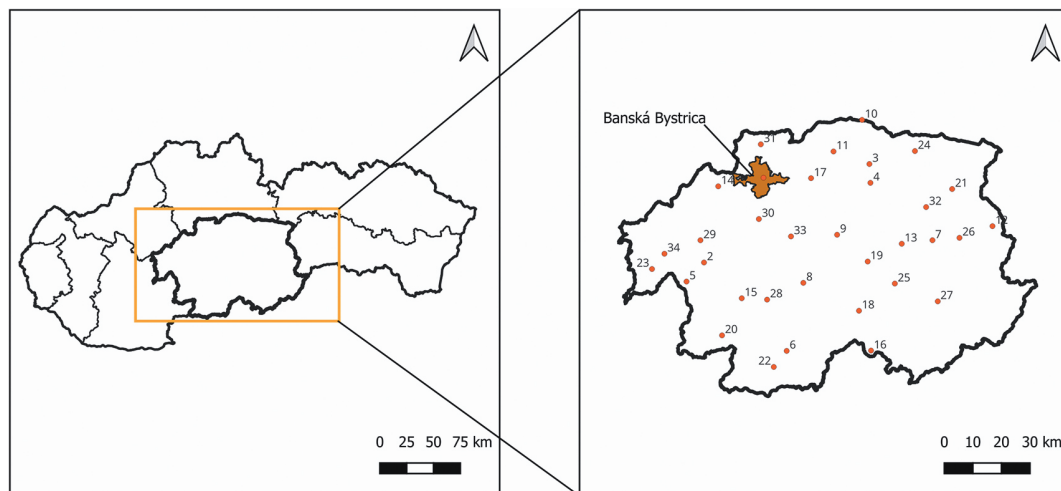
Tab. 1. Gauging stations and their altitudes

| number | gauging station | altitude (m a.s.l.) |
|--------|----------------------|---------------------|
| 1 | Banská Bystrica | 358.30 |
| 2 | Banská Štiavnica | 600.88 |
| 3 | Brezno | 495.49 |
| 4 | Čierny Balog | 533.16 |
| 5 | Dekýš | 466.98 |
| 6 | Dolné Plachtince | 190.08 |
| 7 | Hnúšťa | 365.68 |
| 8 | Horný Tisovnik | 480.65 |
| 9 | Hriňová | 515.19 |
| 10 | Chopok | 2023.97 |
| 11 | Jasenie | 531.98 |
| 12 | Jelšava | 339.39 |
| 13 | Kokava nad Rimavicou | 482.54 |
| 14 | Kremnica | 741.22 |
| 15 | Krupina | 359.41 |
| 16 | Lipovany | 214.79 |
| 17 | Ľubietová | 565.06 |
| 18 | Lučenec | 211.05 |
| 19 | Málinec | 416.29 |
| 20 | Medovárce | 187.02 |
| 21 | Muráň | 458.11 |
| 22 | Nenince | 170.05 |
| 23 | Nová Baňa | 364.25 |
| 24 | Polomka | 635.13 |
| 25 | Poltár | 291.08 |
| 26 | Rátková | 308.10 |
| 27 | Rimavská Sobota | 209.37 |
| 28 | Senohrad | 580.93 |
| 29 | Sklené Teplice | 357.28 |
| 30 | Sliač | 293.37 |
| 31 | Staré Hory | 540.40 |
| 32 | Tisovec | 836.53 |
| 33 | Víglaš | 402.02 |
| 34 | Žarnovica | 313.67 |

Fig. 1. Location of the study area

Explanations:

- 1 – Banská Bystrica,
- 2 – Banská Štiavnica,
- 3 – Brezno,
- 4 – Čierny Balog,
- 5 – Dekýš,
- 6 – Dolné Plachtince,
- 7 – Hnúšťa,
- 8 – Horný Tisovnik,
- 9 – Hriňová,



- 10 – Chopok, 11 – Jasenie, 12 – Jelšava, 13 – Kokava nad Rimavicou, 14 – Kremnica, 15 – Krupina, 16 – Lipovany, 17 – Ľubietová, 18 – Lučenec, 19 – Málinec,
- 20 – Medovárce, 21 – Muráň, 22 – Nenince, 23 – Nová Baňa, 24 – Polomka, 25 – Poltár, 26 – Rátková, 27 – Rimavská Sobota, 28 – Senohrad, 29 – Sklené Teplice,
- 30 – Sliač, 31 – Staré Hory, 32 – Tisovec, 33 – Víglaš, 34 – Žarnovica.

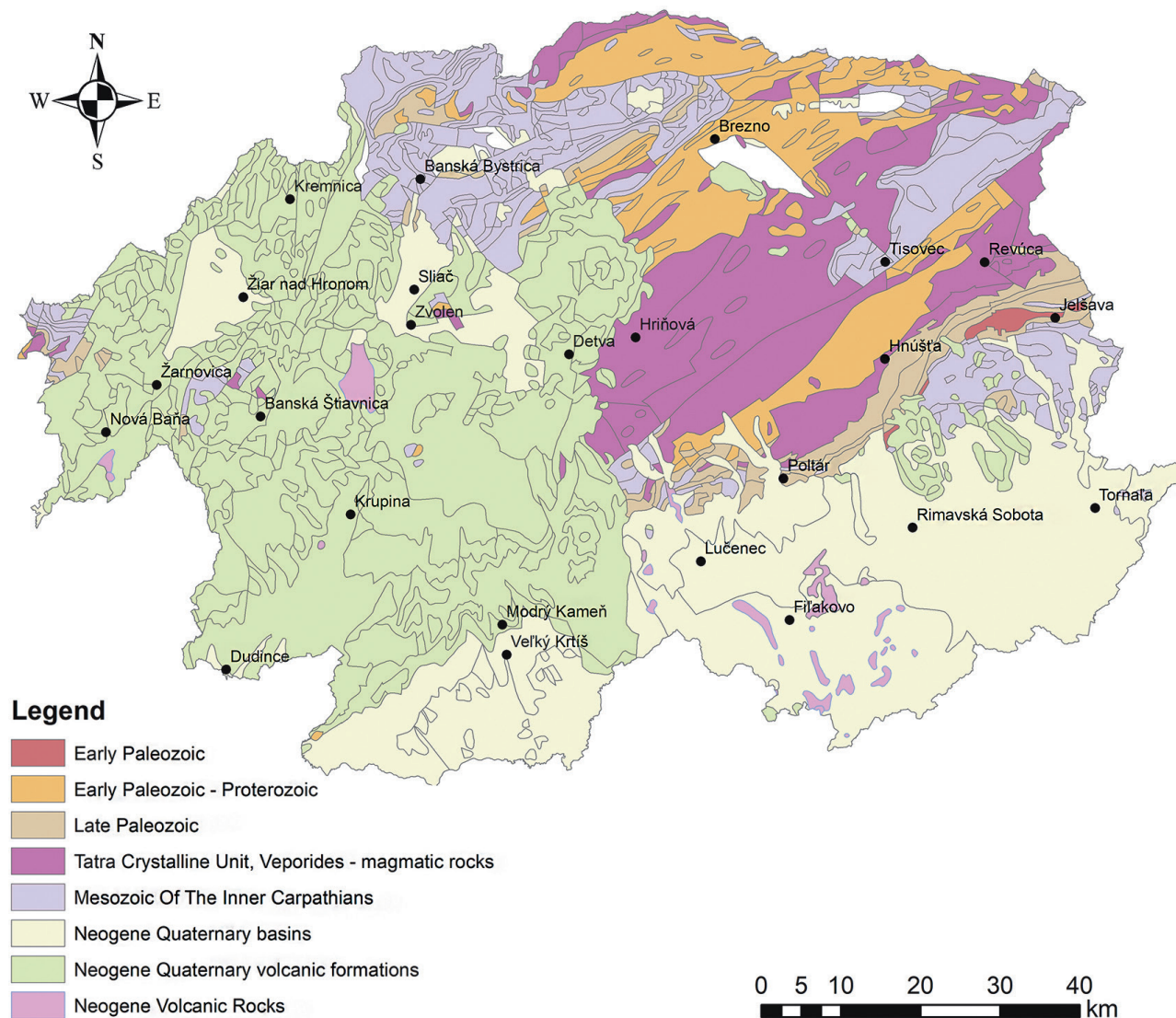


Fig. 2. Geological map of the study area (modified according to Bezák, 2008).

serves as the main water axis of the region. The Ipeľ and Slaná rivers drain the southern and southeastern parts of the territory, with lower discharge due to the dry and warm climate (Atlas of Landscape SR, 2002).

The diversity of orographic and geomorphological features is reflected in the varied geological structure of the region. The geological structure is highly diverse and is illustrated in Figure 2.

Hydrogeological conditions in the area of interest are influenced by the geological structure of the territory, as well as tectonic disturbances, geomorphological, hydrological, and climatic conditions. In the territory of the Banská Bystrica region, all three groups of hydrogeological regions in Slovakia are found, divided according to the determining type of permeability (Atlas of Landscape SR, 2002).

- intergranular permeability (northwest around the Hron River and to the south and southeast of the area),
- karst and karst-fracture permeability (north and east of the area),
- fracture permeability (central part, west, and southeast of the Banská Bystrica region).

The most significant hydrogeological units are represented by Mesozoic rocks and Quaternary cover formations.

3. MATERIAL AND METHODS

3.1. Data

The NASA Prediction of Worldwide Energy Resources (NASA POWER) initiative offers an intuitive online platform for accessing a diverse array of global climate data based on the Modern Era Retrospective-Analysis for Research and Applications (MERRA-2) assimilation products. These resources, accessible at <https://power.larc.nasa.gov/> are curated by the NASA Langley Research Center. The platform provides open-source climate variables, including precipitation. The climate data in NASA POWER primarily originates from the GMAO MERRA-2 assimilation model and the Goddard Earth Observing System (GEOS) 5.12.4 FPIT. Users can explore NASA POWER data at hourly, daily, monthly, annual, and climatological intervals,

with a spatial resolution of 0.5°. Data can be downloaded in various formats such as NetCDF, GeoJSON, ASCII, and CSV for specific regions, periods, and variables, either as single-point or area coverage (Tan et al., 2023). The monthly average precipitation was downloaded in ASCII format for the period from 1981 to 2020, covering 34 gauging stations (Fig. 1, Tab. 1) defined by their geographical latitude and longitude.

3.2. SPI Index

The computation of SPI (Standardized Precipitation Index) is based on a long-term series of monthly precipitation data (a recommended minimum of a thirty-year dataset), transformed using a theoretical probability distribution, most commonly the gamma distribution, into a time series with a normal frequency distribution (Bohniček et al., 2018). In this study, SPI with 6 and 12-month timescales were calculated. To calculate SPI precipitation, data of each station were fitted to a gamma probability distribution function is given (Eq.1) (McKee et al., 1993).

$$g(x) = \frac{x^{\alpha-1} e^{-x/\beta}}{\beta^\alpha \Gamma(\alpha)} \quad (x > 0) \tag{1}$$

α where is the shape parameter, which is estimated using the method of maximum likelihood,

β is the scale parameter, x is the precipitation (mm),

$\Gamma(\alpha)$ is characteristics of the gamma function.

The parameters of the gamma probability distribution function can be expressed following equations (McKee et al., 1993):

$$\alpha = \frac{1}{4A} \left(1 + \sqrt{1 + \frac{4A}{\alpha}} \right), \tag{2}$$

$$\beta = \frac{\bar{x}}{4A'} \tag{3}$$

$$A = \left[\ln(\bar{x}) - \frac{\sum \ln(x)}{n} \right], \tag{4}$$

where A is a dimensionless component used for the calculation of α and β , n is the number of gauging stations, \bar{x} is the average precipitation (mm) for a given month during a statistical period.

The derived parameters enable an efficient representation of precipitation distribution at the station through the utilization of a cumulative mathematical probability function, $G(x)$, as expressed by Eq. 5 (McKee et al., 1993):

$$G(x) = \int_0^x \frac{1}{\beta^\alpha \Gamma(\alpha)} \int_0^x x^{\alpha-1} e^{-x/\beta} dx \tag{5}$$

The cumulative probability function $H(x)$ if $x = 0$ and $q = 0$ probability is given by Eq. 6 (McKee et al., 1993):

$$H(x) = q + (1 - q)G(x) \tag{6}$$

$H(x)$ is subsequently transformed into the standard normal distribution to compute SPI values (McKee et al., 1993; Nasrollahi et al., 2018; Alamdarloo et al., 2020). The SPI Generator software (Nation Drought Mitigation Center, 2018) was used for computing SPI indices in 6 and 12-month time steps, enabling higher precision. After SPI calculation, the classification

of drought severity was performed according to McKee et al. (1993) (Tab. 2).

3.3. Drought hazard

The severity of drought is determined by the duration, intensity, frequency and extent of individual drought episodes. To accurately capture the various aspects of drought, a comprehensive drought hazard assessment model needs to be capable of fully representing these multiple features. The methodological approach for the DHI estimation (Fig. 3) is based on the analysis of the SPI calculated for the drought characterization in the region (Maccioni et al., 2014).

The assessment of drought hazard was calculated based on the probability of drought occurrences. The initial step involved determining the occurrence frequency of diverse drought classes, encompassing moderate, severe, and extremely severe, at each gauging station. Subsequently, the calculation of drought probability within each category allowed for the computation of the percentage probability of drought occurrence in each category.

In the subsequent step of the analysis, point data interpolation was implemented using geostatistical analysis tools, specifically the IDW method within ArcGIS. To quantify the drought hazard, each class was assigned a particular weight as outlined

Tab. 2. SPI classification (McKee et al., 1993)

| Drought category | SPI values |
|--------------------|------------------------------|
| too severe drought | ≤ -2 |
| severe drought | $-1.99 < \text{SPI} < -1.50$ |
| medium drought | $-1.49 < \text{SPI} < -1.00$ |
| normal | $-0.99 < \text{SPI} < 0.99$ |
| medium wet | $1.00 < \text{SPI} < 1.49$ |
| severe wet | $1.50 < \text{SPI} < 2.00$ |
| too severe wet | ≥ 2.00 |

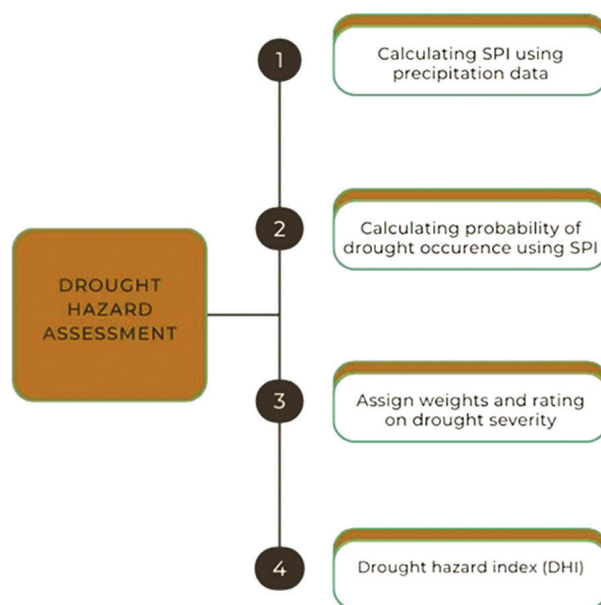


Fig. 3. Procedure used for calculation of drought hazard index (modified according Nasrollahi et al., 2018).

in Tab. 3. In this study, weight 1 was given for normal drought and weight 4 was given for very severe drought as it causes the greatest hazard.

Tab. 3. Weight and rate assigned to drought category

| Drought class | Weight | Rating | Occurrence probability | Area (%) |
|---------------------|--------|--------|------------------------|----------|
| Normal drought | 1 | 1 | ≤ 79.54 | 83.23 |
| | | 2 | 79.54 – 81.34 | 13.43 |
| | | 3 | 81.34 – 82.57 | 2.06 |
| | | 4 | ≥ 83.54 | 1.28 |
| Moderate drought | 2 | 1 | ≤ 6.97 | 43.23 |
| | | 2 | 6.97 – 7.81 | 29.63 |
| | | 3 | 7.81 – 9.08 | 43.23 |
| Severe drought | 3 | 4 | ≥ 11.38 | 1.69 |
| | | 1 | ≤ 5.06 | 35.13 |
| | | 2 | 5.06 – 5.71 | 23.99 |
| | | 3 | 5.71 – 6.49 | 23.93 |
| Very severe drought | 4 | 4 | ≥ 7.32 | 16.95 |
| | | 1 | ≤ 2.28 | 46.2 |
| | | 2 | 2.28 – 2.72 | 29.82 |
| | | 3 | 2.72 – 2.98 | 10.63 |
| | | 4 | ≥ 3.46 | 13.35 |

Assigning values ranging from 1 to 4 was based on the severity of drought groups, namely normal, moderate, severe, and very severe (refer to Tab. 3). The subsequent classification of intensity classes into 4 classes was carried out using the natural break method. This algorithm uses the average of each range for class creation, enhancing data uniformity distribution.

A rate of 1 was given to the class with the lowest percentage probability of drought hazard and a rate of 4 to the class with the highest percentage probability of drought hazard. For instance, in the “Normal drought” class, a rate of 1 corresponds to an occurrence probability ≤ 79.54%, and a rate of 4 corresponds to an occurrence probability ≥ 83.54%. The assigned rates correspond to the severity levels within each drought class, providing a comprehensive assessment of drought intensity. The drought hazard index (DHI) was computed utilizing Eq. 7 and tools of map algebra.

$$DHI = (ND_r * ND_w) + (MD_r * MD_w) + (SD_r * SD_w) + (VSD_r * VSD_w) \quad (7)$$

where ND_r is rating to the normal drought, MD_r is rating to the moderate drought, SD_r is rating to the severe drought, VSD_r is rating to very severe drought, ND_w , MD_w , SD_w and VSD_w are weights for normal, moderate, severe, and very severe drought.

Subsequently, the DHI maps can be categorized into four classes, namely low, moderate, severe, and very severe (Bin et al., 2011; Alamdarloo et al., 2020).

4. RESULTS

For all evaluated stations in the area of interest, an analysis of SPI time series was conducted to examine temporal drought

patterns. SPI time series was displayed on 6- and 12-month scales at selected gauge stations in the investigated area (Fig. 4 and Fig. 5). From the perspective of SPI6 evaluation, it can be noted that the threshold for medium drought (SPI in the range -1.5 to 1.0), with the occurrence of negative SPI-6 values, was exceeded for the Banská Bystrica station in 1995, for the Lučenec station in 1993, for the Kremnica station in 2012, and for the Polomka station, the threshold for medium drought was not exceeded during the assessed period. A significant period with positive SPI-6 values occurred for the Lučenec station in the year 2010, exceeding the threshold for significant wet. In 2010, the threshold for medium wet was exceeded at the Kremnica and Polomka stations. Overall, most monthly precipitation totals remained within or slightly exceeded the normal range.

From the perspective of SPI-12 evaluation, it can be observed that the threshold for medium drought with negative SPI-12 values, was exceeded for the Banská Bystrica station in 1995 and 2014, for the Lučenec station in 1993 and 2012, for the Kremnica station in 1993 and 2012, and for the Polomka station in 1984 and 2012. A significant period with positive SPI-12 values occurred for the Banská Bystrica station in 2012, for the Lučenec and Kremnica stations in 2010, and for the Polomka station in the years 2010 and 2020. Overall, most monthly precipitation totals remained within or slightly exceeded the normal range.

The results of the evaluation for the 4 investigated stations (Fig. 4 and Fig. 5) demonstrate a certain temporal correlation. It can be noted that certain differences in the temporal correlation among all evaluated precipitation stations are primarily caused by variations in elevation, ranging from 126 to 2043 meters above sea level, leading to uneven precipitation distribution. While the results of the case study for the stations used in this work are somewhat correlated with the time series, the overall results of the time series indicate the occasional occurrence of droughts in all examined stations. The SPI method can be used to determine the areas and extent of potential drought.

To assess the spatial distribution of drought hazard, was created a map depicting the probability of drought occurrence, referred to as the Drought Hazard Index (DHI) (Fig. 6). The DHI for each assessed station is listed in Table 4.

The Drought Hazard map is characterized by a value interval which defines the degree of drought probability in a given area. The sum value interval of the final map was divided according to the “natural breaks” classification method implemented in the

Tab. 4. DHI of assessed stations

| DHI | Gauging station |
|-----------|--|
| very low | Banská Štiavnica, Dekýš, Kremnica, Krupina, Medovárce, Nová Baňa, Sklené Teplice, Žarnovica |
| low | Brezno, Hnúšťa, Chopok, Jasenie, Jelšava, Kokava nad Rimavicou, Múráň, Poltár, Rátková, Rimavská Sobota, Staré Hory, Tisovec |
| high | Banská Bystrica, Čierny Balog, Ľubietová, Lučenec, Málinec, Senohrad, Sliač, Vigláš |
| very high | Dolné Plachtince, Horný Tisovník, Hriňová, Lipovany, Nenince, Polomka |

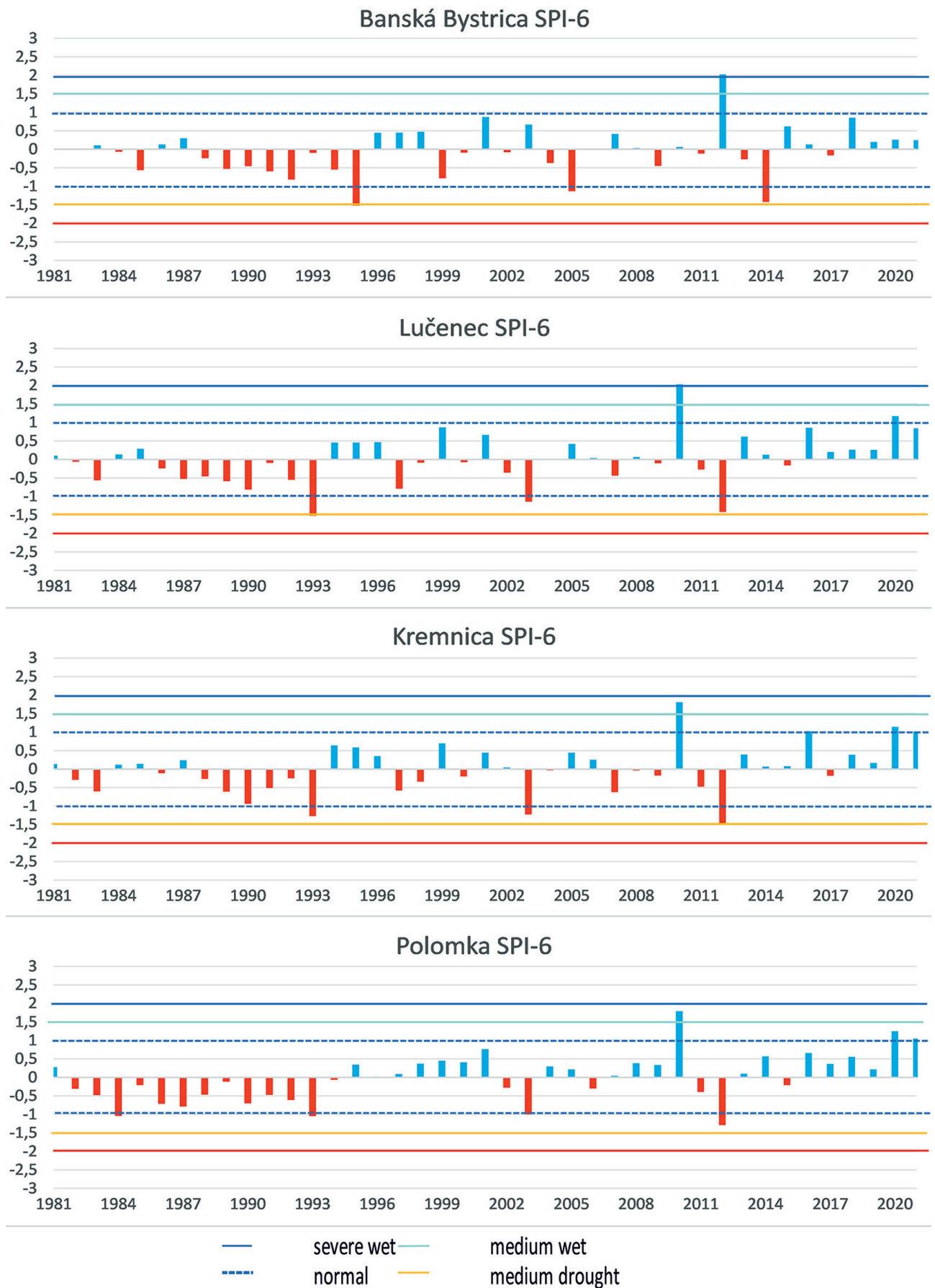


Fig. 4. Graphic evaluation of SPI-6 for selected stations during the specified period.

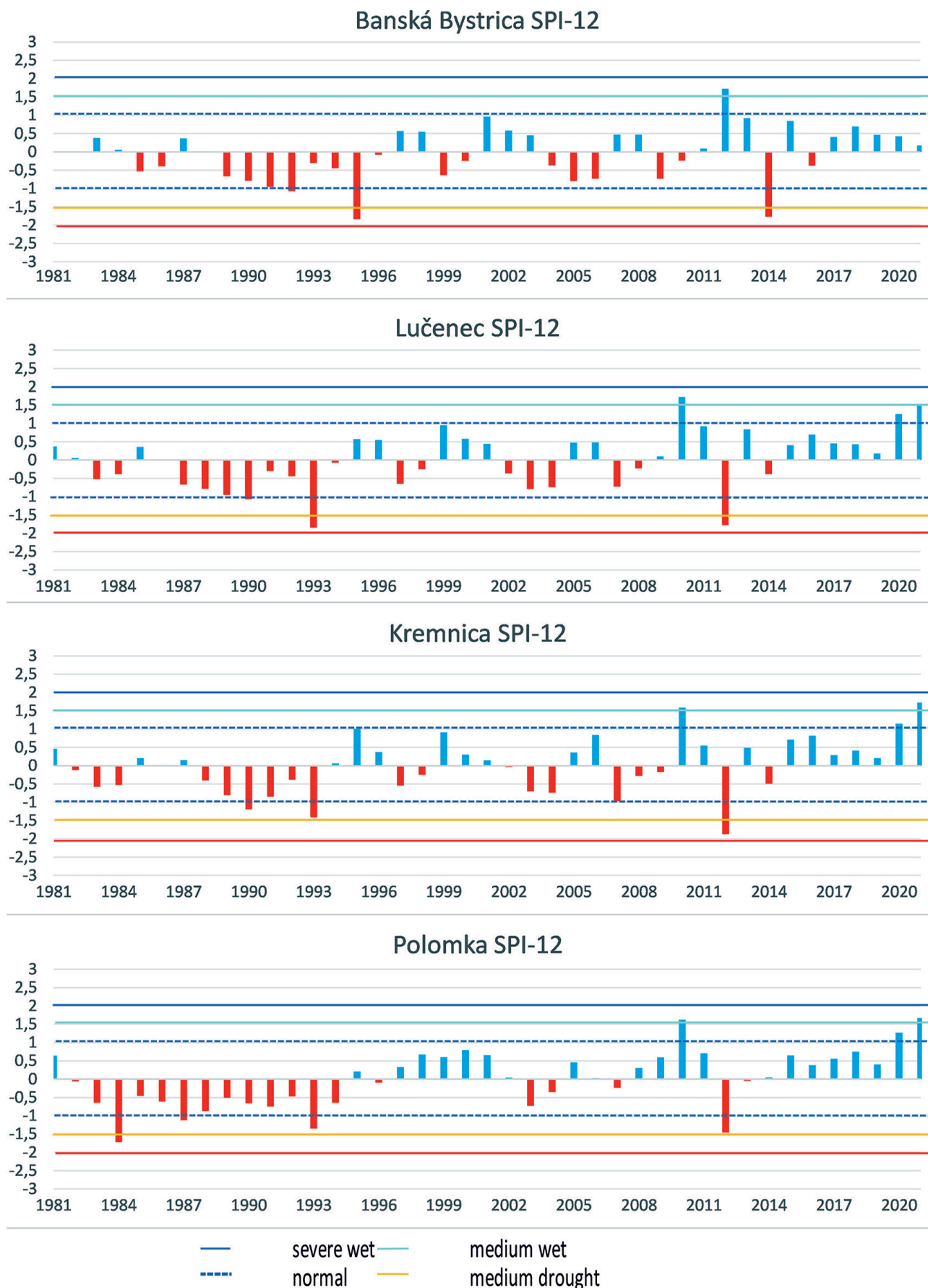


Fig. 5. Graphic evaluation of SPI-12 for selected stations during the specified period.

ArcGIS environment. The drought hazard map was reclassified into four classes, which express very low, low, medium, and very high probabilities. The second class is found the largest extent. The spatial distribution of areas within different drought hazard classes is delineated by the following percentages: 29.19% of the area resides in the very low class, 33.52% in the low class, 24.86% in the high class, and 12.42% in the highest, very high class. This distribution elucidates the heterogeneous susceptibility to drought across the evaluated region, with a substantial portion categorized as low risk, while a smaller part of territory has a heightened risk of drought hazard.

The spatial analysis of drought hazard distribution indicates that the severity of drought hazard is particularly high in the southeastern to southern part of the region and in the northeastern part of the area. The combination of factors such as topographical features, land use patterns, and climatic conditions contributes to the heightened susceptibility of these areas to drought events. This is influenced by the intricate interplay of geographic elements, human activities, and prevailing weather conditions, collectively amplifying the risk of drought in the southeastern to southern part of the region and in the northeastern portion of the area.

5. DISCUSSION

The aim of this study was a comprehensive assessment of drought in the Banská Bystrica region, utilizing a combination of the Standardized Precipitation Index (SPI) and Geographic Information Systems (GIS). With the largest area in Slovakia, the Banská Bystrica region provides a representative area for studying drought due to its geological diversity, altitude, and varying hydrogeological conditions.

The evaluation of 34 precipitation stations in the region, utilizing data from the NASA POWER platform for the period 1981–2020, allowed for an in-depth assessment of the impact of precipitation on drought occurrence. However, Tan et al. (2023) highlighted the need to consider data bias in NASA POWER, which can lead to underestimation of precipitation and maximum temperature and overestimation of minimum temperature. Nevertheless, NASA POWER remains a valuable tool for exploring the spatial and temporal dynamics of climate variables.

To illustrate drought assessment using SPI indices, stations in Banská Bystrica, Kremnica, Lučenec, and Polomka were selected (Fig. 4 and Fig. 5). However, the lack of temporal correlation among all evaluated stations was attributed to significant

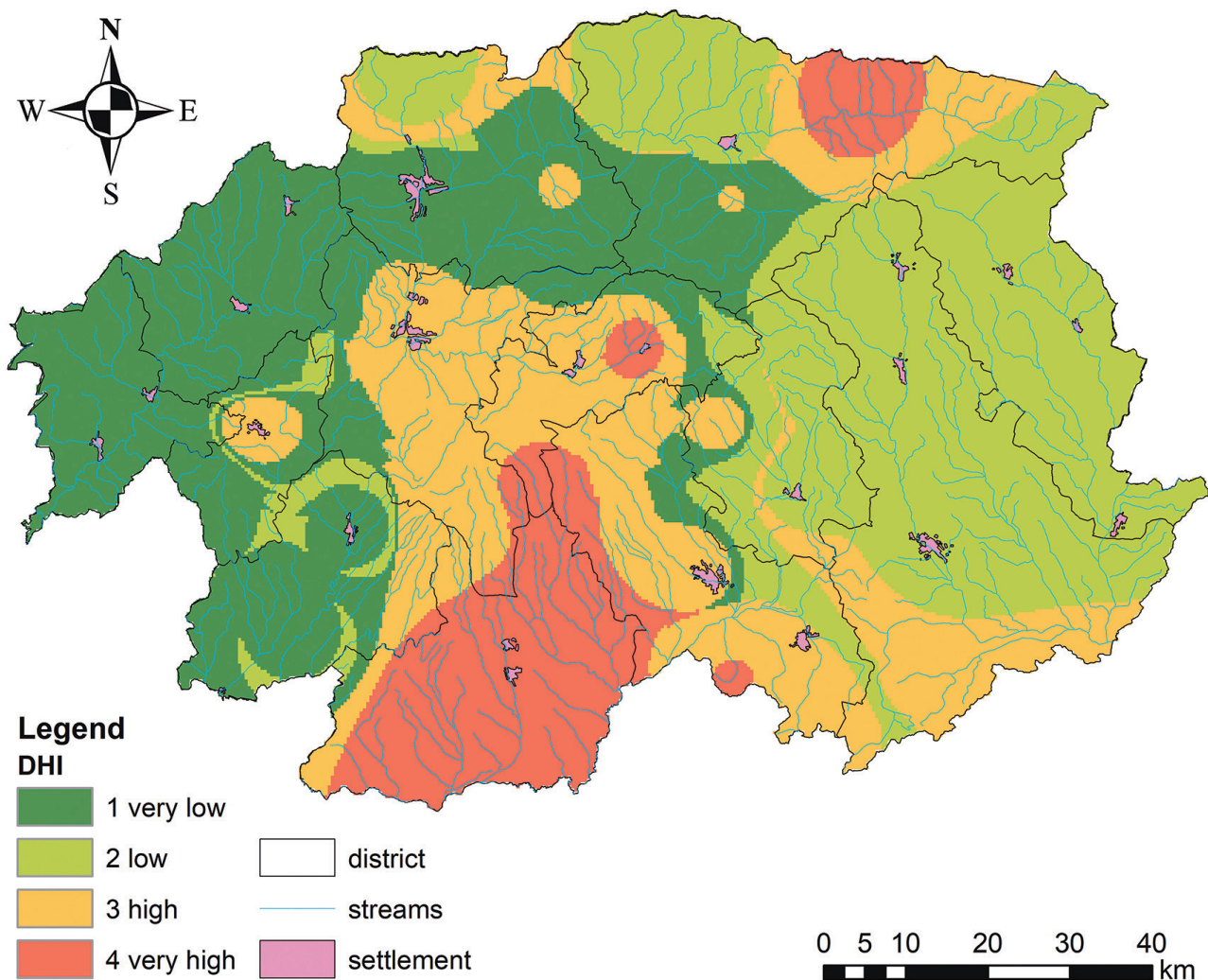


Fig. 6. Map of drought hazard index.

differences in elevation and, consequently, varying precipitation distribution.

Spatial characteristics of drought, explored by Bin (2011) et al. and Angelidis et al. (2011) provided insights into regions prone to drought and the suitability of probability distributions. Subsequently, a comprehensive Drought Hazard map was created for the entire area of interest, categorizing it into four classes based on SPI values, drought occurrence probabilities, weight assignments, and severity ratings.

6. CONCLUSION

The paper aligns with current trends in drought assessment by combining meteorological methods with advanced GIS techniques. The ArcMap environment served as a robust framework for analyses and modeling, laying the groundwork for future climate and drought research.

The study emphasized the importance of continuous refinement of assessment methods to better understand and predict the complex processes of climate change impact on drought. The final perspective highlighted GIS as an effective tool for quantifying, identifying, and predicting the impacts of climate change on drought. A comprehensive analysis, including the vulnerability and risk assessment, contributes to a better understanding of dynamic droughts and defines vulnerable areas, providing essential tools for water resource management and protection.

Acknowledgements: This research was funded by the Slovak Research and Development Agency under contract No. APVV-14-0174, as well as the Ministry of Education, Science, Research and Sport of the Slovak Republic under contract No. VEGA 1/0302/21.

References

- Alamdarloo E. H., Khosravi H., Nasabpour S. & Gholami A., 2020: Assessment of drought hazard, vulnerability and risk in Iran using GIS techniques. *Journal of Arid Land*, 12, 6, 984–1000.
- Angelidis P., Maris F., Kotsovinos N. & Hrisanthou V., 2012: Computation of drought index SPI with alternative distribution functions. *Water Resources Management*, 26, 2453–2473.
- Asrari E., Masoudi M. & Hakimi S. S., 2012: GIS overlay analysis for hazard assessment of drought in Iran using Standardized Precipitation Index (SPI). *Journal of Ecology and Field Biology*, 35, 4, 323–329.
- Atlas of Landscape of the Slovak Republic, 2002: 1st edition. Ministry of Environment SR, Bratislava, Slovak Environmental Agency, Banská Bystrica, 344 p. [in Slovak]
- Bezák V., Elečko M., Fordinál K., Ivanička J., Kaličiak M., Konečný M., Maglay J., Mello J., Nagy A., Porfaj M., Biely A., Bóna J., Buček S., Filo I., Gazdačko L., Grecula P., Gross P., Havrila M., Hók J., Hraško L., Jacko S., Janocko J., Kobulský J., Kohut M., Kováčik M., Lexa J., Madaras J., Nemeth Z., Olšovský M., Plašienka D., Pristaš J., Rakús M., Salaj J., Siman P., Šimon L., Teťák F., Vass D., Vozár J., Vozarova A. & Zec B., 2018: Prehľadná geologická mapa Slovenskej republiky 1:200 000. [General Geological Map of the Slovak Republic, 1:200 000] [online] State Geological Institute of Dionýz Štúr in Bratislava. Available on internet: <https://apl.geology.sk/pgm/>.
- Bin H., Aifeng L., Jianjun W., Lin Z. & Ming L., 2011: Drought hazard assessment and spatial characteristics analysis in China. *Journal of Geographical Sciences*, 21, 2, 235–249.
- Dabanli I., 2018: Drought hazard, vulnerability, and risk assessment in Turkey. *Arabian Journal of Geosciences*, 11, 18, 538.
- Domonkos P., 2003: Recent Precipitation Trends in Hungary in the Context of Larger Scale Climatic Changes. *Natural Hazards*, 29, 255–271.
- Bochníček O., Blaškovičová L., Damborská I., Fendek M., Fendeková M., Horvát O., Pekárová P., Slivová V. & Vrablíková D., 2018: Prognosis of Hydrological Drought development in Slovakia. Comenius University Bratislava, Bratislava, 182 p.
- Hajar H. A. A., Murad Y. Z., Shatanawi K. M., Al-Smadi B. M. & Hajar Y. A. A., 2019: Drought assessment and monitoring in Jordan using the standardized precipitation index. *Arabian Journal of Geosciences*, 12, 14, 417.
- Janáčova T., Labudová L. & Labuda M., 2018: Meteorologické sucho v oblastiach Slovenska s nížinným charakterom v rokoch 1981–2010. *Geographia Cassoviensis*, 12, 1, 53–64. [in Slovak with English abstract]
- Lana X., Rodriguez-Sola R., Martinez M. D., Casas-Castillo M. C., Serra C & Kirchner R., 2021: Autoregressive process of monthly rainfall amounts in Catalonia (NE Spain) and improvements on predictability of length and intensity of drought episodes. *International Journal of Climatology*, 41, S1, 178–194.
- Maccioni P., Kossida M., Brocca L. & Moramarco T., 2014: Assessment of the Drought Hazard in the Tiber River Basin in Central Italy and a Comparison of New and Commonly Used Meteorological Indicators. *Journal of Hydrologic Engineering*, 20, 8, 05014029.
- McKee T. B., Doesken N. J. & Kleist J., 1993: The relationship of drought frequency and duration of time scales. In: *Waldstreicher J. (Ed.) Bulletin of the American Meteorological Society, Eighth Conference on Applied Climatology, American Meteorological Society, 17–22 January 1993*, 179–186.
- Nagy P., Purcz P., Galas S., Portela M. M., Hlavatá H. & Simonová D., 2020: Trend analysis of drought indices in the eastern Slovakia. In: *Carter C. B. (Ed.) IOP Conference Series: Materials Science and Engineering 867, October 2020, High Tatras, Slovakia*, 1–5.
- Nam W. H., Hayes M. J., Svoboda M. D. & Tadesse T., 2015: Drought hazard assessment in the context of climate change for South Korea. *Agricultural Water Management*, 160, 10–12, 106–117.
- Nasrollahi M., Khosravi H., Moghaddamnia A., Malekian A. & Shahid S., 2018: Assessment of drought risk index using drought hazard and vulnerability indices. *Arabian Journal of Geosciences*, 11, 20, 606.
- Portela M. M., Zelenáková M., Santos J. F., Purcz P., Silva A. T. & Hlavatá H., 2015: A comprehensive drought analysis in Slovakia using SPI. *European Water*, 51, 15–31.
- Rahman R. & Lateh H., 2016: Meteorological drought in Bangladesh: assessing, analysing and hazard mapping using SPI, GIS and monthly rainfall data. *Environmental Earth Science*, 75, 12, 1026.
- Rozkošný J., Ivaňáková G., Mrekaj I., Turňa M., Labudová L., Krčová I., Špilda I., Ridzoň J. & Mikulová K., 2022: Analýza vplyvu sucha na lesné porasty v regióne Oravy v období 2015–2021. In: *Kunca A. (Ed.) Aktuálne problémy v ochrane lesa, October 2023, Grandhotel Bellevue, Horný Smokovec*, 1–12.
- Salvacion A. R., 2021: Multiscale drought hazard assessment in the Philippines. In: *Pourghasemi H. R. (Eds.) Computers in Earth and Environmental Sciences*, chapter 11, Elsevier; 1st edition, pp. 169–179.
- Tan M. L., Armanuos A. M., Ahmadianfar I., Demir V., Heddam S., Al-Areeq A. M., Abba S. I., Kilinc H. C. & Yaseen Z. M., 2023: Evaluation of NASA POWER and ERA5-Land for estimating tropical precipitation and temperature extremes. *Journal of Hydrology*, 624, 129940.

- Tsesmelis D. E., Vasilakou C. G., Kalogeropoulos K., Stathopoulos N., Alexandris S. G., Zervas E., Oikonomou P. D. & Karavitis C., 2022: Drought assessment using the standardized precipitation index (SPI) in GIS environment in Greece. In: In: Pourghasemi H. R. (Eds.) *Computers in Earth and Environmental Sciences*, chapter 46, Elsevier; 1st edition, pp. 619–633.
- Turňa M., Ivaňáková G., Krčová I., Mrekaj I. & Ridzoň J., 2021: Zhodnotenie sucha na Slovensku v roku 2020. *Meteorologický časopis*, 24, 1, 11–20. [in Slovak with English abstract]
- Wilhite D. A., 2005: Drought and water crises. Science, technology and management issues. Taylor & Francis, 108 p.